Thermodynamic analysis of $Fe_{72}Pt_{28}$ Invar

Bernd Rellinghaus, Jochen Kästner, Thomas Schneider, and Eberhard F. Wassermann
Labor für Tieftemperaturphysik and SFB166, Gerhard-Mercator-Universität Duisburg, 47048 Duisburg, Federal Republic of Germany

Peter Mohn
Institut für Elektrochemie, Technische Universität Wien, A-1060 Wien, Austria
(Received 19 August 1994)

We present measurements of the specific-heat capacity $c_p(T)$ and the thermal expansion coefficient $\alpha(T)$ on ordered and disordered $Fe_{72}Pt_{28}$ Invar in the temperature range $4 < T < 1200$ K. In a detailed discussion of the various contributions to the total specific-heat we show that after properly correcting for the thermal expansion of the alloy, the specific-heat anomaly around the Curie temperature in ordered $Fe_{72}Pt_{28}$ is sharper than in the disordered alloy. The results for the magnetic specific heat are compared with theoretical finite-temperature expansions of the $T = 0$ band structure for Fe_3Pt, exhibiting pronounced moment-volume instabilities. In accordance with the theoretical predictions we find that the magnetic contribution to the specific heat in the paramagnetic range decreases with increasing temperature, and thus seems to be dominated by strong spin fluctuations. However, the jump in $c_p(T)$ at T_C observed in the model calculations is not supported by our experiments. From a comparison of the total measured specific heat with $c_p(T)$ of a fictitious, nonmagnetic reference material we estimate the energy, which stabilizes the magnetic Invar phase, to be about 1 mRy/atom. This is comparable to the energetic stability of the fcc austenitic phase as compared to the bcc martensitic phase.

I. INTRODUCTION

During the past years there has been considerable progress in the understanding of moment-volume instabilities (MVI's) in a certain group of fcc $3d$ transition-metal alloys showing a broad spectrum of magnetovolume anomalies, which form the so-called Invar effect, when the electron concentration lies in the critical range $e/a = 8.5-8.7$.[1–3] To date, the ground-state properties of these systems are well understood through *ab initio* theoretical calculations of the total energy as a function of the atomic volume and moment, $E(V, M)$. Characteristic is the occurrence of two distinct magnetic states [two minima in the $E(V, M)$ plane], the so-called high-spin (HS) state with a high magnetic moment and the low-spin (LS) state with a low moment, respectively.[4–9] For Invar systems, the ground state is the ferromagnetic (FM) HS state at large volumes, separated by an energy difference of about 1 mRy from the LS state at smaller volume. The LS state exhibits antiferromagnetic order in FeNi Invar and FM order in FePt Invar. Systems with reversed order of states, i.e., for which the LS state at small volumes is the ground state, are called "anti-Invar" systems.[10–12] Experimental evidence for a transition from the HS to the LS state in $Fe_{72}Pt_{28}$ Invar by pressure has been given in Mößbauer experiments at 4.2 K.[13]

The distortion in the $E(V, M)$ plane due to the formation of a second minimum causes an additional "magnetic anharmonicity," which affects the equilibrium volume of the respective alloy. Extensions of the $T = 0$ band-structure calculations to finite temperatures using a phenomenological Ginzburg-Landau (GL) formalism[14–16] reveal that in Invar systems this anharmonicity effect is negative and results in a partial compensation of the normal positive thermal expansion of the lattice, which is represented by a Grüneisen behavior. In anti-Invar systems just the opposite is found. These alloys exhibit a positive magnetic anharmonicity and show an enhanced thermal expansion at high temperatures.[10–12,17] However, in spite of many efforts, the physical nature of the thermal excitations in systems with MVI is still not understood. The reason is the lack of a detailed knowledge of the electron-phonon coupling mechanism, allowing for an understanding of the moment-volume fluctuations. Moreover, the influence of existing long-range magnetic order remains an open question. In a theoretical GL formalism systems with MVI anomalies show a first-order transition at the respective ordering temperatures; in the experiments this is not the case.

To shed more light on this situation, we present in this paper experimental data of the specific heat and the thermal expansion coefficient of ordered and disordered $Fe_{72}Pt_{28}$ Invar, measured in the broad temperature range $0 < T < 1200$ K, from far below to far above the respective Curie temperatures T_C. We show that the magnetic contribution to the specific heat decreases with increasing temperature in the range above T_C, in accordance with theoretical predictions from finite-temperature GL calculations. From the enthalpy difference between $T = 0$ and $T > T_C$, determined from the anomalous contribution to the specific heat as compared to that of a "normal" metal, some information about the energy difference between the HS and the LS state in the FePt Invar will be

derived and compared with the theoretical predictions, too. Finally, an analysis of the Gibbs free energy as a function of temperature allows us to understand the phase stability of the ordered phase with respect to the disordered one and, in a similar fashion, the relative energetic stability of the austenitic fcc phase against the martensitic bcc phase in this alloy system.

II. EXPERIMENT

The specific-heat measurements are carried out in a quasiadiabatic pulse calorimeter in the temperature range 300 K$\leq T \leq$ 1200 K. Figure 1 shows a schematic drawing of the calorimeter cell. To achieve satisfactory accuracy we use big cylindrical samples (S) of 60 mm in length and 20 mm in diameter, weighing approximately 230 g. A bifilar heater (H), wound around a supporting element made of hot presssed boron nitride (HPBN) is fixed in a central bore, which is closed by means of a screw made of sample material to ensure that the generated heat stays within the sample. The sample is held in position by means of the four wires of the heating element (H), insulated with Al_2O_3 microcapillaries, and fed through four holes in the top of the sample. The temperature is measured with a $Pt/Pt_{87}Rh_{13}$ thermocouple (TC), placed in a 20-mm-deep pinhole in the sample. An automatically controlled ice bath is used as a reference. Using a $6\frac{1}{2}$ digit nanovoltmeter, we reach a temperature resolution of better than 2 mK. The surfaces of the sample are polished to reduce the total emissivity. The sample is surrounded by an active radiation shield (RS) made of HPBN. The inner and outer surfaces of the shield are covered with 25 μm molybdenum foil to reduce radiation coupling with the sample and the surrounding tube oven, respectively. Two differential thermocouples (DT1 and DT2) allow us to keep the radiation-shield temperature within ± 0.1 K of the surface temperature of the sample, even during a heat pulse. In a similar way the auxiliary plate (AP) (made of HPBN) compensates for the losses via all the wires connected with the sample. All wires are thermally anchored to this plate. As shown in Fig. 1, the cell is placed into a temperature-controlled oven (O). The Al_2O_3 tube of the oven is evacuated to a pressure of $p_{end} \leq 10^{-5}$ mbar prior to an experimental run to reduce the oxygen. Measurements are done in a pure Ar atmosphere with a typical pressure of $p = 10$ mbar.

The specific heat can be measured in three different ways, by using (i) the conventional heat-pulse method, (ii) a continuous-mode method, in which the specific heat is determined from the time derivative of the sample temperature, and (iii) a relaxation-time method, in which the temperature of the surrounding environment is kept constant, and the sample temperature relaxes towards it after application of a heat pulse. We remark that the results obtained from all three methods for the same sample differ by no more than $\pm 1.5\%$, which also represents the reproducibility of our experiments.

To demonstrate the absolute accuracy and reliability of our setup we show in Fig. 2 the results of the specific heat (full dots and inset) as measured on pure iron as a reference material. For $T < T_C$ our data agree very well with those taken from the literature.[18–22] Obviously, there is disagreement in absolute values of $c_P(T)$ at higher temperatures $T \geq 1000$ K, a result that indicates the problem of calibrating any specific-heat experiment in this range

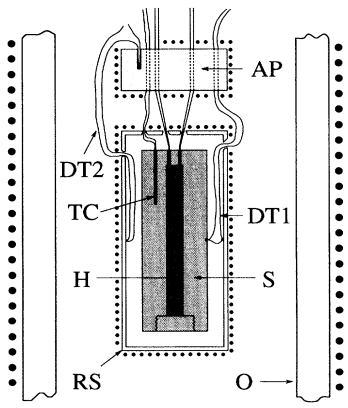

FIG. 1. Schematic drawing of the calorimeter cell consisting of the sample (S), sample thermocouple (TC), two differential thermocouples (DT1 and DT2), the auxiliary plate (AP), the active radiation shield (RS) made of HPBN, the heating element (H) (HPBN), and the surrounding tube oven (O).

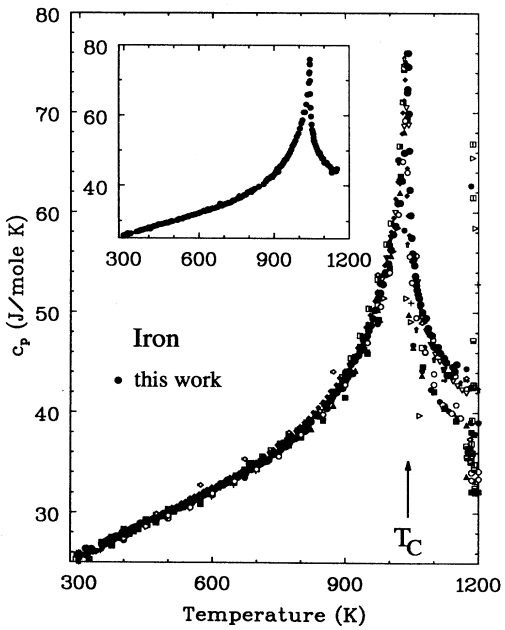

FIG. 2. Specific heat, c_p, of pure iron vs temperature. A comparison of our results separately plotted in the inset with various data as taken from the literature (Refs. 18–22) reveals a good agreement in the range $T < 1000$ K. At higher temperatures different data scatter by up to 10%. The decrease of c_p at $T = 1183$ K originates from the structural α(bcc) $-$ γ(fcc) phase transition.

because of lack of a reliable and well-established reference material (sapphire, the National Bureau of Standards (NBS) standard, is hardly machinable to achieve the sample geometry necessary here). Note the drop in the specific heat of Fe because of the γ-α structural transition at the $A3$ point of 1183 K.

III. SAMPLE PREPARATION

The $Fe_{72}Pt_{28}$ sample is prepared by means of induction melting in an Al_2O_3 crucible under Ar atmosphere using 99.98% Fe and 99.95% Pt as primary materials. The alloy is kept in the liquid state for about 2 h before the crucible is lowered out of the high-frequency coil with a velocity of 20 mm/h. The concentration and homogeneity are checked by means of energy-dispersive x-ray investigations to agree with the nominal value within 0.3 at.%. The mean concentration is determined to be $Fe_{71.9}Pt_{28.1}$. After being machined to the required geometry the sample is sealed in a quartz tube under a 200-mbar argon atmosphere. The ordered state ($L1_2$) is obtained by the following annealing sequence: 1 h at T=900 °C, 1 h at T=800 °C, 1 day at T=700 °C, 4 days at T=600 °C, 10 days at T = 500 °C, 1 month at T=450 °C, cooling to room temperature. The disordered sample is annealed at T=930 °C for 3 h and then quenched in water, thereby distroying the quartz tube. The degree of order is determined by x-ray diffraction experiments. For the ordered sample we obtain $S \geq 0.9$; the disordered sample reveals no Cu_3Au-type superstructure peaks at all. Using tungsten powder as a reference, the lattice contants at 300 K are determined to be a = 3.751 Å for the ordered and a = 3.748 Å for the disordered sample, respectively.

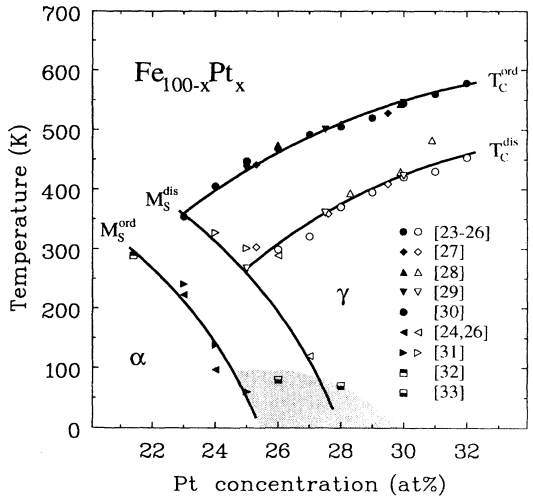

FIG. 3. Phase diagram of $Fe_{100-x}Pt_x$ around the stoichiometric composition Fe_3Pt. T_C^{ord} and T_C^{dis} denote the Curie temperatures of the ordered and disordered alloys, respectively. M_S^{ord} and M_S^{dis} denote the martensite start temperatures. The M_S lines separate the fcc(γ) and bcc(α) stability regions. In the hatched area premartensite is assumed to appear in the ordered phase (Ref. 33).

The magnetic transition temperatures are determined from resistivity measurements and the temperature dependence of the magnetization in small fields. We obtain T_C^{ord} = 505±5 K and T_C^{dis} = 355±5 K in good agreement with the phase diagram[23–33] given in Fig. 3.

IV. RESULTS OF THE SPECIFIC-HEAT MEASUREMENTS

Figure 4(a) shows the total specific heat $c_p(T)$ of ordered (full dots) and disordered (open dots) $Fe_{72}Pt_{28}$ versus temperature. Data in the range 4.2–300 K, earlier measured by Schubert,[34] fit very well to the high-temperature (HT) results as achieved within this work. The electronic contributions as determined from the low-temperature (LT) behavior are represented by the linear coefficients γ_{LT}^{ord} = 9.7 mJ mole^{-1}K^{-2} and γ_{LT}^{dis} = 7.9 mJ mole^{-1}K^{-2}. The respective Debye temperatures increase with temperature from Θ_{LT}^{ord} = 200 K at T = 4.2 K to Θ_{HT}^{ord} = 318 K at $T \geq$ 75 K for the ordered sample and from Θ_{LT}^{dis} = 225 K to Θ_{HT}^{dis} = 300 K for the disordered $Fe_{72}Pt_{28}$.[34,35] Note the anomalous behavior

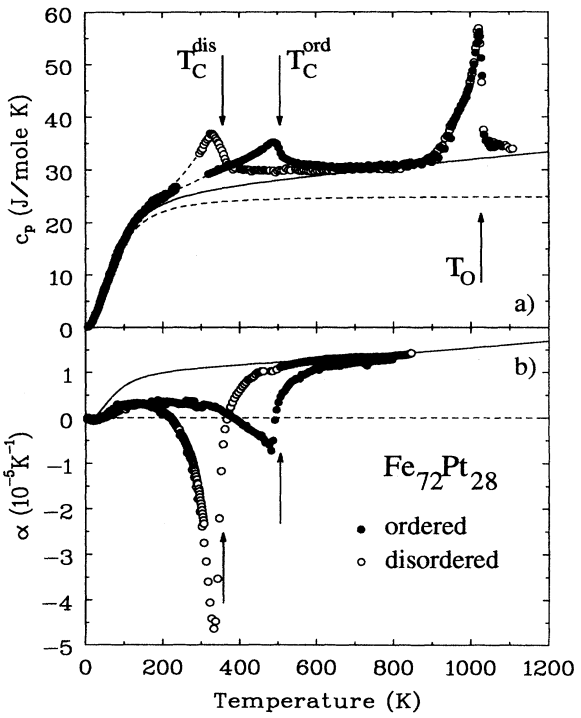

FIG. 4. (a) Specific heat c_p of ordered and disordered $Fe_{72}Pt_{28}$ vs temperature. The dashed line shows a Debye-type phononic contribution, c_v^{Debye} (Θ_D = 318 K). The solid line represents the specific heat of a nonmagnetic reference material, which neither exhibits an Invar anomaly nor an order-disorder transition. The arrows indicate the Curie temperatures T_C and the ordering temperature T_O. (b) Thermal expansion coefficient α as a function of T for the same alloys as shown in (a). In the HT range data can be described by a normal metallic Grüneisen behavior with Θ_D = 318 K (solid line).

of $c_p(T)$ in the vicinity of T_c, where for both the ordered and the disordered samples we observe relatively broad and rounded maxima, definitely not typical for a second-order magnetic phase transition. Note further that the maxima in $c_p(T)$ do not coincide with the respective T_c's. Similar features in the specific heat around T_c have been observed on other Invar alloys.[36–38]

To demonstrate that the observed anomalies are caused by thermal excitations typical for systems with MVI's, we show in Fig. 4(b) the thermal expansion coefficient α as measured as function of temperature on the same alloys. A comparison between the two figures immediately reveals the correlation between both physical properties. Both types of anomalies, the one in $c_p(T)$ and the one in $\alpha(T)$, occur simultaneously, exactly within the same temperature range and in the vicinity of T_c for both alloys. Note that the minima in $\alpha(T)$, like the maxima in c_p, do not lie at T_c. These observations prove that the anomalies in $c_p(T)$ and $\alpha(T)$ are caused by the same type of thermal excitations and are of the same physical nature. The anomalous behavior is certainly not bound to the specific heat and thermal expansion alone but are found in other physical properties (elastic constants, bulk modulus, forced volume magnetostriction), too.[1] Currently, however, the respective excitations (moment-volume fluctuations or "elastomagnons") are not understood microscopically, as already mentioned above.

Referring back to Fig. 4(a), we see that with increasing temperature in the range above T_c the specific heat of the ordered and the disordered alloy shows an anomalously "flat" behavior, i.e., hardly any further increase, until at temperatures $T > 900$ K there is the onset of the order-disorder transition with a sharp maximum at $T_O = 1022$ K. This value is in good agreement with $T_O = 1000$ K found for $Fe_{75}Pt_{25}$ by Pepperhoff,[39] but significantly lower than the value of $T_O \simeq 1108$ K published by Hansen and Anderko.[40]

It might be striking that an order-disorder transition is also observed for the disordered alloy. However, this is a consequence of our experimental procedure. It takes about one week to measure the specific heat of a sample in the range from 300 to 1200 K. Consequently, even the disordered sample is slowly stepwise annealed and successively ordered during the measurement. The effect is made plausible in Fig. 5, where the temperature dependence of the order parameter S (full curve) is shown schematically as a function of temperature for a system with $L1_2$ super structure. S jumps to zero at the critical temperature T_O because this phase transition is of first order.[41] Since the disordered state is thermodynamically a nonequilibrium state, its order parameter $S_{\rm dis}$ (dashed curve) increases with temperature, starting from a small, arbitrarily chosen value at $T = 0$. Depending on the heating velocity, $S_{\rm dis}$ will match the equilibrium order parameter S at a temperature somewhat below T_O, but finally the initially disordered alloy will undergo the order-disorder phase transition, too. Though the peak width in $c_p(T)$ at T_O found experimentally is relatively small, we do not observe a latent heat within the ordering range. This is probably due to the large mass of our samples, allowing for small temperature gradients during a heat pulse smearing out the phase transition.

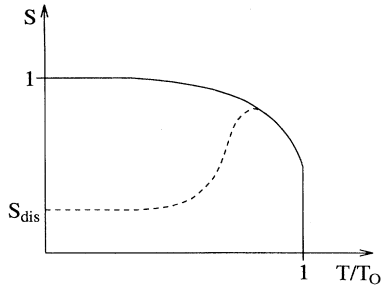

FIG. 5. Schematic drawing of the temperature dependence of the order parameter S of an ordered system with $L1_2$ superstructure (solid line). The dashed line shows the temperature dependence of $S_{\rm dis}$ for a disordered alloy with an arbitrarily choosen value at $T = 0$. With increasing temperature $S_{\rm dis}$ is assumed to successively approach the equilibrium value S at a temperature smaller than T_0.

V. ANALYSIS OF THE SPECIFIC-HEAT DATA

As mentioned in the Introduction, in MVI systems, electrons and phonons are closely coupled. Since a satisfactory theoretical description of the coupling at finite temperatures is still lacking, we assume—as in normal metals—the respective contributions to the specific heat to be additive. c_p is thus given by the sum of the following terms:

$$c_p = c_v^{\rm Debye} + c_v^{\rm el} + c_v^{\rm mag} + (c_p - c_v). \tag{1}$$

Contributions originating from the order-disorder transitions are not taken into consideration here. $c_v^{\rm Debye}$ is the phononic part described within the framework of a Debye model, $c_v^{\rm el}$ the electronic specific heat, $c_v^{\rm mag}$ the magnetic specific heat, and $c_p - c_v$ the contribution due to the thermal expansion of the alloy. In the following we discuss these various contributions to the specific heat on the basis of our experimental results.

A. Specific heat due to thermal expansion

Using first-principles thermodynamic relations,[42] the contribution of the volume expansion (or contraction) can be calculated from the thermal expansion coefficient, α, the molar volume, $V_{\rm mol}$, and the adiabatic bulk modulus, B_s, respectively:

$$c_p - c_v = c_p \left(1 - \frac{1}{1 + \frac{9\alpha^2 V_{\rm mol} B_s T}{c_p}} \right). \tag{2}$$

Equation (2) reveals that $c_p - c_v$ is dominated by the temperature dependence of the thermal expansion coefficient $\alpha(T)$.

Values for the adiabatic bulk modulus B_S of disordered $Fe_{72}Pt_{28}$ can be derived from the elastic constants C_L, C', and C_{44} as determined in sound velocity measurements by Hausch[43] using

$$B_S = C_L - \frac{C'}{3} - C_{44}. \tag{3}$$

The respective evaluation for the ordered sample is done by using C_L data from Hausch,[43] while C' and C_{44} are taken from inelastic neutron-scattering experiments by Tajima *et al.*[44] The results for $c_p - c_v$ are plotted in Fig. 6.

As is to be expected, $c_p - c_v$ behaves strongly anomalously around T_C. Starting from high temperatures, data first decrease almost linearly for both types of order and then drop to zero when the thermal expansion vanishes. The minima in $\alpha(T)$ on further decreasing the temperature [cf. Fig. 4(b)] yield maxima in $c_p - c_v$, specifically pronounced for the disordered sample, where $\alpha(T)$ reaches a large negative value of -4.7×10^{-5} K^{-1} at $\simeq 330$ K.

B. Phononic specific heat

The phononic contributions to the specific heat are treated within the Debye model. The temperature-dependent Debye temperature Θ_D, which is the essential parameter that fully specifies $c_v^{\text{Debye}}(T)$, has been determined in the earlier LT specific-heat measurements by Schubert.[34] The respective values, $\Theta_{\text{HT}}^{\text{ord}} = 318$ K and $\Theta_{\text{HT}}^{\text{dis}} = 300$ K (see Sec. IV) lead, within accuracy limits, to the same dependence of $c_v^{\text{Debye}}(T)$ for both types of order [cf. dashed curve in Fig. 4(a)].

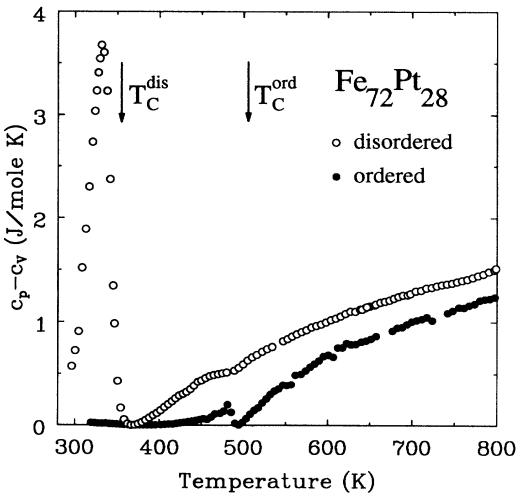

FIG. 6. Temperature dependence of the contribution to the specific heat originating from the thermal expansion $(c_p - c_v)$ for ordered (full points) and disordered (open points) $Fe_{72}Pt_{28}$. The arrows indicate the Curie temperatures.

C. Electronic specific heat

A first approximation for the electronic specific heat at HT can be done by assuming the magnetic contribution to the specific heat to vanish at $T \gg T_C$. That this is a reasonable assumption is supported by the results of $\alpha(T)$ in Fig. 4(b), showing that $\alpha(T)$ can be described by a Grüneisen curve in the HT range for $T \gg T_C$, i.e., the magnetic contributions are negligible here. The electronic specific heat can then be determined from Eq. (1):

$$c_p - c_v^{\text{Debye}} - (c_p - c_v) = c_v^{\text{el}} = \gamma_{\text{HT}} T \tag{4}$$

under the assumption that c_v^{el} is linear in T in the HT range.

A reference line, suitable to determine the magnetic contribution to the specific heat (c_v^{mag}, see below) and simultaneously leading to quantitative values of γ_{HT}, can now be found in the following way. Disregarding the effects caused by the ordering, we assume that the sum of the contributions $c_v^{\text{Debye}} + c_v^{\text{el}} + (c_p - c_v)$ is equal to the experimentally determined specific heat c_p at temperatures roughly around 850 K. This leads to $\gamma_{\text{HT}}^{\text{ord}} = 4.6$ mJ mole^{-1} K^{-2} for the ordered and $\gamma_{\text{HT}}^{\text{dis}} = 4.4$ mJ mole^{-1} K^{-2} for the disordered sample. The respective reference lines are shown in Fig. 7 in the range from 300 to 800 K for the two samples.

A comparison with the LT values[34] of $\gamma_{\text{LT}}^{\text{ord}} = 9.7$ mJ mole^{-1} K^{-2} and $\gamma_{\text{LT}}^{\text{dis}} = 7.9$ mJ mole^{-1} K^{-2} reveals that there are considerable reductions of the electronic specific heat with increasing temperature in both states

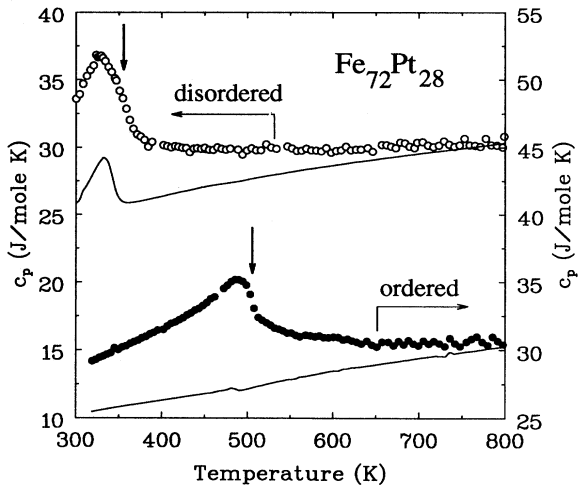

FIG. 7. Specific heat c_p vs temperature [data as taken from Fig. 4(a)] in the range $300 < T < 800$ K for ordered (full points) and disordered (open points) $Fe_{72}Pt_{28}$. The arrows indicate the Curie temperatures. The full lines are the reference lines as determined from the sum of the Debye contribution c_v^{Debye} [cf. dashed curve in Fig. 4(a)], the thermal expansion $c_p - c_v$ (from Fig. 6), and an electronic contribution c_v^{el}, which can be determined under the assumption that the magnetic contribution to the specific heat vanishes in the range $T > 800$ K. (For further details see text.)

of the alloy. These differences may arise from electron-phonon (EP) interactions, which lead to an enhancement of the LT coefficient $\gamma_{LT} \equiv \gamma(T=0)$:[45]

$$\gamma(T) = [1+\lambda(T)]\gamma_{bare} = \left(1+\lambda_0 \frac{\gamma_{ep}(T)}{\gamma_{ep}(0)}\right)\gamma_{bare}. \quad (5)$$

Here, λ denotes the EP mass enhancement factor, with a temperature dependence given by a function $\gamma_{ep}(T)/\gamma_{ep}(0)$ as taken from Grimvall.[45] γ_{bare} denotes the nonenhanced coefficient determined by the electronic density of states (DOS) at the Fermi energy $N(E_F)$:

$$\gamma_{bare} = \frac{\pi^2}{3} k_B^2 N(E_F). \quad (6)$$

If the observed differences between the HT and the LT electronic specific-heat coefficients are fully attributed to EP interactions, we can determine from Eq. (5) γ_{bare} and λ_0 by using our experimental values of γ_{HT} and γ_{LT} as reference points. The resulting temperature dependence of $\gamma(T)$ for ordered $Fe_{72}Pt_{28}$ is shown as an example in Fig. 8(a), where c_v^{el}/T versus T is plotted together with γ_{LT}^{ord} (full point) and γ_{HT}^{ord} (horizontal bar). From a plot of $c_v^{el}(T)$ in Fig. 8(b) it can be seen that, despite of the temperature dependence of $\gamma(T)$, a linear behavior in the form $c_v^{el}(T) = \gamma_{HT}T$ is a good approximation to describe the electronic specific heat even down to temperatures $T \simeq 100$ K. The fits lead to $\gamma_{bare}^{ord} = 5.1$ mJ mole^{-1} K^{-2} and $\lambda_0^{ord} = 0.9$ for ordered $Fe_{72}Pt_{28}$, and $\gamma_{bare}^{dis} = 4.8$ mJ mole^{-1} K^{-2} and $\lambda_0^{dis} = 0.65$ for the disordered sample. Of course, the corrected γ_{bare} values should be equivalent to the electronic DOS at the Fermi level rather than γ_{HT}. Recent theoretical calculations[46] yield $\lambda_0^{theor} = 0.5$ for ordered Fe_3Pt (the respective value for the disordered alloy is not available), thus revealing a sizable difference in comparison to the experimental value of $\lambda_0^{ord} = 0.9$ for ordered $Fe_{72}Pt_{28}$. All γ and λ values are collected in Table I.

For comparison of the electronic γ with theory we also show in Table I values for γ_{bare}^{theor}, which are calculated by means of Eq. (6) from the respective DOS.[47,48] There is accordance between experiment and theory with respect to the fact that the γ values are always larger in the ordered state as compared to the disordered one. From Table II, where the available theoretical DOS data for FePt- and FeNi-Invar alloys are shown, it can be seen that a similar difference between the ordered and the disordered state results for Fe_3Ni. However, as Table

TABLE I. Comparison between the experimental and the theoretical values of the coefficients of the electronic specific heat, γ (in mJ mole^{-1} K^{-2}), and the EP enhancement factor, λ_0, for $Fe_{72}Pt_{28}$.

Sample	γ_{LT}	γ_{HT}	γ_{bare} [a]	γ_{bare}^{theor} [b]	λ_0	λ_0^{theor} [b]
Ordered	9.7	4.6	5.1	3.1	0.9	0.5
Disordered	7.9	4.4	4.8	2.7	0.65	-

[a]Derived from a fit of Eq. (5) to γ_{LT} and γ_{HT}.
[b]Calculated for Fe_3Pt.

TABLE II. Electronic DOS at the Fermi level, $N(E_F^0)$, taken from results of theoretical band-structure calculations (see references in the table). The coefficients of the electronic specific heat γ_{bare} are evaluated from Eq. (6) for $T = 0$.

Alloy[a]	State[b]	$N(E_F^0)$ (Ry^{-1} atom^{-1})	γ_{bare} (mJ mole^{-1} K^{-2})	Ref.
Fe_3Pt (o)	HS	17.6	3.0[c]	47
	HS	18.2	3.1	48
Fe_3Pt (d)	HS	15.8	2.7	48
Fe_3Ni (o)	HS	21.1	3.6	56
	HS	22.4	3.8	8
	LS	21.4	3.7	8
Fe_3Ni (d)	HS	15.2	2.6	56
$Fe_{60}Ni_{40}$ (d)	HS	14.6	2.5	56

[a](o) and (d) mean the ordered and disordered alloys, respectively.
[b]HS denotes the high-spin ground state and LS the low-spin state.
[c]The value given in Ref. 47 is divided by 4, since the author takes $4N_A$ atoms per mole, while we take N_A atoms per mole.

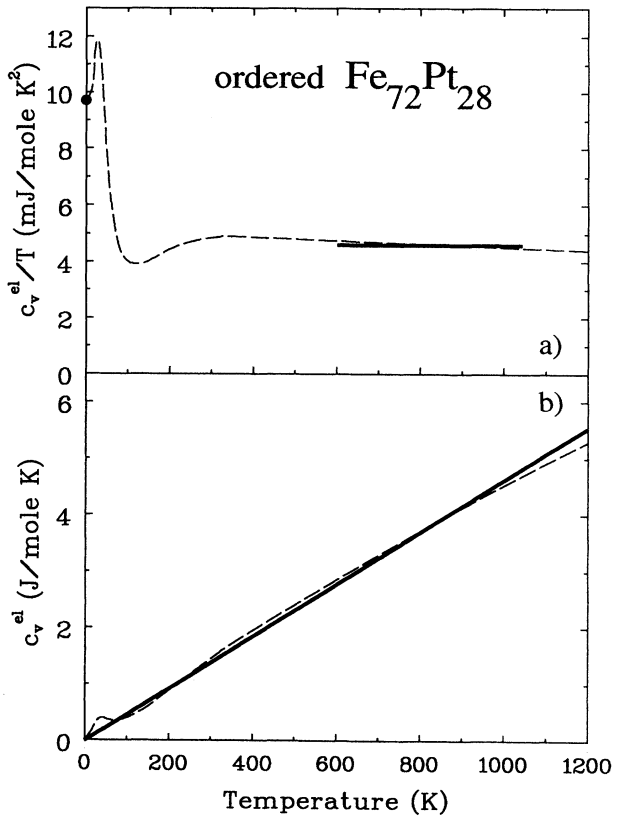

FIG. 8. Electronic contribution c_v^{el} to the specific heat of ordered $Fe_{72}Pt_{28}$. (a) Temperature dependence in the form $\gamma(T) = c_v^{el}/T$ vs T (dashed line) resulting from a fit of Eq. (5) to values of γ_{LT} (full dot) and γ_{HT} (horizontal bar). (b) Resulting electronic contribution c_v^{el} for γ_{HT} (solid line) and after Eq. (5) (dashed line).

I reveals, the theoretical values $\gamma_{\text{bare}}^{\text{theor}}$ are significantly smaller than the respective experimental ones. Changes in the electronic DOS at E_F of Invar alloys can occur if, at finite temperatures, the low-spin (LS) state instead of the high-spin (HS) state determines the electronic properties, and thereby the DOS. Unfortunately, theoretical data of $N(E_F)$ for the LS state in Fe_3Pt are not available in the literature. Calculations on ordered Fe_3Ni, on the other hand, exhibit no difference between the DOS for the HS state and the LS state at E_F (cf. Table II). Therefore, the discrepancies between $\gamma_{\text{bare}}^{\text{theor}}$ and γ_{bare} from experiment are unlikely to originate from the reversal of the states. They rather call for additional contributions to the specific heat at HT, such as by anharmonic vibrations or complex electronic excitations coupled to the volume of the system.

Finally we remark that further temperature-dependent effects on the electronic specific heat can arise from the temperature dependence of the coefficient γ_{bare} itself. However, this rather results in a reduction of the DOS at E_F, thus increasing the discrepancy between the experimental and theoretical findings.

D. Magnetic specific heat

Following the above discussion (cf. Sec. V C), the magnetic contributions to the specific heat result from the difference between the experimental $c_p(T)$ data and the respective reference curves (cf. Fig. 7). Data for ordered (full points) and disordered (open points) $Fe_{72}Pt_{28}$ are plotted versus the temperature in Fig. 9(a). As a consequence of the strongly anomalous thermal expansion, the magnetic anomaly of the disordered sample appears much sharper than for the disordered one.[49] In an earlier publication,[50] $(c_p - c_v)$ was assumed to be linear in temperature even around T_C, and thus led to magnetic anomalies sharper for the disordered than for the ordered $Fe_{72}Pt_{28}$ sample. This could not be explained, since disorder is expected to smear out the magnetic phase transition rather than order. The contradiction is now resolved by the present investigations through properly taking into account $c_p - c_v$.

It is obvious from Fig. 9(a) that large magnetic contributions to the specific heat remain at temperatures well above the Curie temperature T_C. We think that these originate from moment-volume fluctuations. To support this assumption, we show in Fig. 9(b) the magnetic contribution c_v^{mag} divided by its maximum value $c_{\text{max}}^{\text{mag}}$ versus the reduced temperature T/T_C. The solid line represents the theoretical result from Mohn, Schwarz, and Wagner.[51] It is obtained from an expansion of the zero-temperature band-structure results to finite temperatures, predicting contributions to the specific heat from spin and volume fluctuations in the range $T > T_C$. A similar finding has been published by Schröter, Entel, and Mishra.[52] Though theory and experiment disagree in the range around and below the Curie temperature, they are in accordance within the range above T_C. Thus, the experiments support the theoretical finding that there is an almost linear *decrease* in the magnetic specific heat

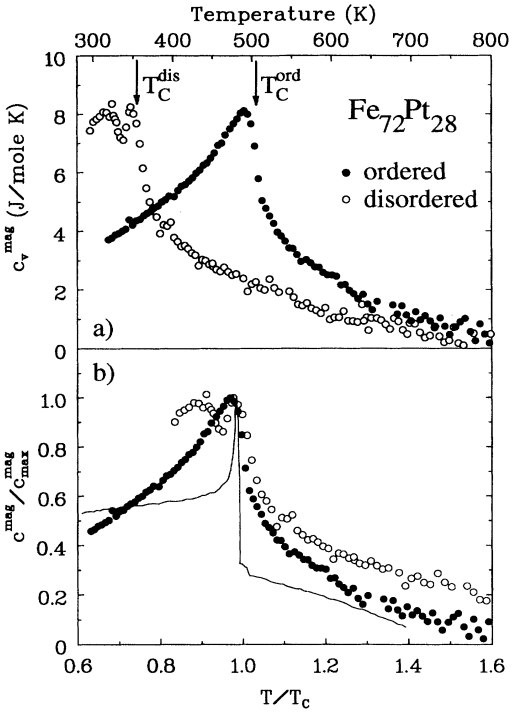

FIG. 9. (a) Magnetic contribution to the specific heat c_v^{mag} of ordered and disordered $Fe_{72}Pt_{28}$ vs temperature. Data result from Fig. 7 by subtracting the reference line $[c_v^{\text{Debye}} + c_v^{\text{el}} + (c_p - c_v)]$ from the measured $c_p(T)$ data. Note that a considerable magnetic heat capacity remains in the paramagnetic temperature range. The arrows indicate the Curie temperatures. (b) Reduced plot of the magnetic heat c_v^{mag} divided by its maximum value $c_{\text{max}}^{\text{mag}}$ vs T/T_C. The solid line represents the theoretical result of Mohn, Schwarz, and Wagner (Ref. 51).

with rising temperature. This contribution originates from spin fluctuations dominating the contribution from the volume fluctuations and appears to be typical for Invar systems.

Theoretical calculations on Invar always exhibit very flat minima in the total energy surfaces $E(M,V)$, defining the ground state of the alloy. It is thus suggestive to assume that a supply of little energy to the system allows for large moment fluctuations. However, the finite-temperature calculations based on a classical GL approach have to be handled with care, since sometimes they yield unphysical properties such as a negative entropy.[52,15]

VI. PHASE STABILITY CONSIDERATIONS

A. Magnetovolume enthalpy

To work out Invar typical energies from the specific heat it is necessary to find a respective nonmagnetic reference *not* exhibiting any Invar anomaly. Since such a material does not exist, we choose the following proce-

dure. It is well established that the Invar anomalies in the thermal expansion, the elastic constants, or the specific heat occur below and around the respective Curie temperature of an Invar system but vanish in the range far above T_C.[1] Thus, we can assume that in the high-temperature range $T \gg T_C$ the behavior of the (hypothetical) reference material and the respective Invar alloy are equal. Provided, the Debye temperature, the electronic, and expansion contribution are the same in both materials, the heat capacity of the reference material is then given by

$$c_p^{\text{ref}} = c_v^{\text{Debye}} + c_v^{\text{el}} + (c_p - c_v). \tag{7}$$

In first approximation, all contributions but the phononic one vary linearly with temperature. Since Θ_D is known from the LT data, we can now fit the specific heat of the reference material to the experimental data of the alloy in such a way that both match in the HT range, disregarding the effects caused by the ordering. The result is shown in Fig. 4(a) by the full curve, the "pure" Debye contribution by the dashed curve.

On the basis of this result we now can determine the excess enthalpy, necessary to heat an Invar alloy to a given temperature, as compared to the enthalpy for the respective nonmagnetic reference. Since the excess specific-heat capacity is given by the relation

$$c^{\text{ex}} = c_p - c_p^{\text{ref}}, \tag{8}$$

the corresponding excess enthalpy H^{ex} results from

$$H^{\text{ex}}(T) = \int_0^T c^{\text{ex}}(\tau) d\tau. \tag{9}$$

Figure 10 shows the result of this calculation for the ordered $Fe_{72}Pt_{28}$ sample (full curve) and the disordered sample (dashed curve). As can be seen from the figure, the excess enthalpy at T_C is about 1 mRy/atom (right-hand scale) for both samples. Moreover, enthalpy and internal energy are about equal, since they only differ by $\int (c_p - c_v) dT$, which is a small correction. As a consequence, we find the important result that the excess internal energy is of the same order of magnitude as the energy difference between the HS and the LS state. Theoretical values (for $T = 0$) for ordered Fe_3Pt are $\Delta E_{\text{HS-LS}} =$ 1 mRy/atom (Ref. 52) and $\Delta E_{\text{HS-LS}} = 1.2$ mRy/atom (Ref. 53). Though thermal excitation processes in Invar are far from being understood, we remark that finite-temperature calculations have shown that, neglecting the normal lattice anharmonicity, in ordered Fe_3Pt the HS ground-state develops into the LS state, when the temperature is raised from $T = 0$ to the Curie temperature.[52] As a consequence, the assumption lies close that both quantities describe the same physical property, namely, the energy difference necessary to excite an Invar system from the HS ground state to the LS state in the range from $T = 0$ to $T = T_C$.

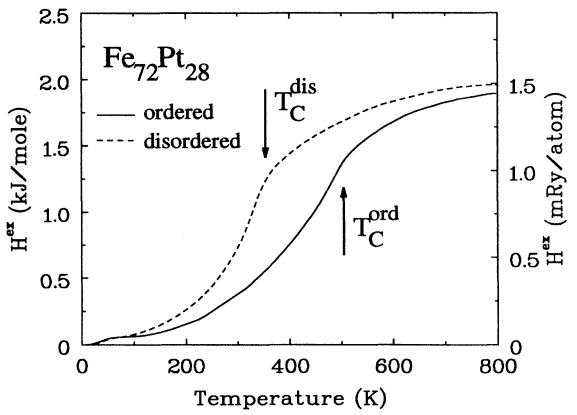

FIG. 10. Excess enthalpy of ordered and disordered $Fe_{72}Pt_{28}$ as derived from experimental specific heat data. The arrows denote the magnetic transition temperatures.

B. Order-disorder enthalpy

In an analogous way we can find the energy difference, which stabilizes the $L1_2$ ordered structure with respect to the disordered one. To account for the fact that, due to the experimental procedure, the disordered sample also undergoes the order-disorder transition, $H^{\text{dis}}(T)$ is corrected by means of a free-hand extrapolation for temperatures $T > 850$ K. The enthalpies of the ordered and disordered alloy are shifted then in a way that they match at temperatures above the ordering temperature T_O, where the difference between $H^{\text{ord}}(T)$ and $H^{\text{dis}}(T)$ vanishes. Besides additional constant contributions from the zero-point enthalpies, we can then calculate the respective enthalpies by integrating the specific heat of the ordered and disordered $Fe_{72}Pt_{28}$. The resulting $H(T)$ data are plotted in Fig. 11(a).

For determination of the respective Gibbs free enthalpy curves, the entropy $S(T)$ is needed. It can be calculated from the relation

$$S^{\text{ord/dis}}(T) = \int_0^T \frac{c_p^{\text{ord/dis}}(\tau)}{\tau} d\tau + S_0^{\text{ord/dis}}. \tag{10}$$

The resulting Gibbs free enthalpy is shown in Fig. 11(b). Note that the origins of the scales for $H(T)$ and $G(T)$ in Fig. 11 are arbitrarily chosen because of the nondetermined additive integration constants. Since at $T = 0$ the difference in the Gibbs free enthalpy $\Delta G^{\text{ord-dis}}(T = 0)$ and $\Delta H^{\text{ord-dis}}(T = 0)$ are identical, we obtain the experimental result that an energy of 1.2 mRy/atom stabilizes the ordered phase with respect to the disordered one. This is comparable to theoretical results of Kuhnen and Da Silva,[54] who calculated $\Delta G^{\text{ord-dis}}(T = 0) =$ 1.67 mRy/atom for ordered ($L1_2$) Fe_3Pd.

C. fcc-bcc instability

To achieve an estimate for the energy, which stabilizes the fcc phase with respect to the bcc phase, $\Delta G^{\text{fcc-bcc}}(T = 0)$, we make use of the above derived re-

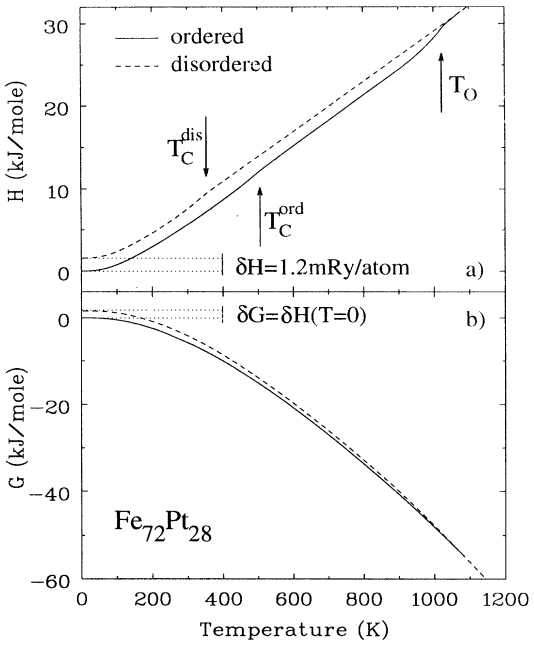

FIG. 11. (a) Enthalpy $H(T)$ and (b) Gibbs free enthalpy $G(T)$, as functions of the temperature for ordered (full line) and disordered (dashed line) $Fe_{72}Pt_{28}$. For both thermodynamic potentials, the data of the ordered and the disordered sample are set equal at temperatures above the ordering temperature T_O. Note that at $T = 0$ the difference in the Gibbs free enthalpy, $\Delta G(T = 0) = G^{ord} - G^{dis}$, is equal to the enthalpy difference, $\Delta H(T = 0)$. The arrows indicate the Curie temperatures T_C and the ordering temperature T_O. The origins of the H and G axes are chosen arbitrarily.

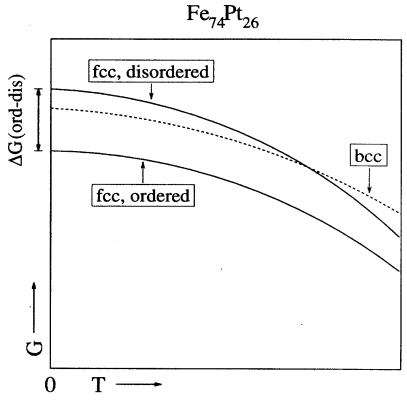

FIG. 12. Schematic drawing of the temperature dependence of the Gibbs free enthalpy for the fcc-ordered phase G^{ord}, the fcc-disordered phase G^{dis}, and the bcc phase G^{bcc} (dashed curve), for $Fe_{74}Pt_{26}$. The relative position of G^{ord}, G^{dis}, and G^{bcc} is determined from the phase diagram given in Fig. 3.

sult for the difference in the Gibbs free enthalpy between the ordered and the disordered phase, $\Delta G^{ord\text{-}dis}(T = 0)$. For $Fe_{72}Pt_{28}$ the ordered phase turns out to be the thermodynamic equilibrium phase. As a consequence, its Gibbs free enthalpy, $G^{ord}(T)$, is smaller than $G^{dis}(T)$ at all temperatures below the ordering temperature T_O. Since both the ordered and the disordered alloys do not undergo a martensitic transformation to $T = 0$, the curve $G^{bcc}(T)$ must lie above $G^{dis}(T)$ and $G^{ord}(T)$ for all temperatures.

From the phase diagram (Fig. 3) it can be seen that for $Fe_{74}Pt_{26}$ the ordered phase is fcc down to $T = 0$, while the disordered alloy becomes bcc at an M_S temperature somewhat below room temperature. Therefore, evidently the Gibbs free enthalpies of $Fe_{74}Pt_{26}$ behave as schematically sketched in Fig. 12. Here, we restrict our considerations to temperatures below the ordering temperature of the system. Similarly to the $Fe_{72}Pt_{28}$, the ordered fcc phase is the overall thermodynamic equilibrium phase. Thus, $G^{ord}(T)$ exhibits the smallest absolute values as compared to any other Gibbs free enthalpy. The disordered phase, on the other hand, is separated energetically from the ordered one by the enthalpy difference $\Delta H^{ord\text{-}dis}(T = 0)$. For $Fe_{72}Pt_{28}$ we know that $\Delta H^{ord\text{-}dis}(T = 0) = 1.2$ mRy/atom. It is reasonable to assume and known from experimental data on $Fe_{75}Pt_{25}$ (Ref. 39) that the order-disorder enthalpy difference hardly changes when varying the concentration by $2 - 3$ at. %. [However, it does not affect the argumentation to allow for a 50% uncertainty in $\Delta H^{ord\text{-}dis}(T = 0)$.] Thus we can deduce that the difference in the Gibbs free enthalpy between the ordered and the disordered $Fe_{74}Pt_{26}$ also amounts to $\Delta G^{ord\text{-}dis} \simeq 1.2$ mRy/atom.

Since disordered $Fe_{74}Pt_{26}$ undergoes a martensitic transformation, while the ordered alloy remains fcc, the Gibbs free enthalpy curve for the bcc phase $G^{bcc}(T)$ must lie between $G^{dis}(T)$ and $G^{ord}(T)$ at temperatures below the martensite start temperature M_S^{dis}. Here, we do not distinguish between a bcc-ordered and a bcc-disordered phase, since the bcc lattice cannot carry any 3:1 order. Furthermore, the martensitic transformation is strongly inhomogeneous and does not allow for long range order in the martensite. However, differences between $G^{bcc,ord}$ and $G^{bcc,dis}$ cannot be excluded, but are assumed to be negligible for the current discussion.

This confinement condition for $G^{bcc}(T = 0)$ allows us to determine an upper limit for the fcc-bcc stabilizing energy:

$$\Delta G^{fcc\text{-}bcc}(T = 0) \leq 1.2 \text{ mRy/atom}. \qquad (11)$$

Recent theoretical investigations on ordered Fe_3Ni (Ref. 55) reveal that the energy difference between the fcc and the bcc structure is ~ 1.6 mRy/atom, thus claiming for the tendency of the Invar to exhibit a structural and a magnetovolume instability side by side. Similar calculations on Fe_3Pt are still lacking.

VII. SUMMARY AND CONCLUSION

We have measured the specific heat $c_p(T)$ and the thermal expansion coefficient $\alpha(T)$ of ordered and disordered

$Fe_{72}Pt_{28}$ in the temperature range 4–1200 K. In a detailed analysis we deal with the c_p data as consisting of additive contributions $c_v^{\text{Debye}} + c_v^{\text{el}} + c_v^{\text{mag}} + (c_p - c_v)$ originating from phonons, which are treated within a Debye model, electrons, the magnetism, and the expansion of the lattice, respectively. We have shown that the largely negative thermal expansion coefficient of disordered $Fe_{72}Pt_{28}$ around the Curie temperature T_C causes a strong anomaly in $c_p - c_v$. This sizable contribution explains the previously unresolved problem of a sharper maximum in the total specific heat for the disordered sample as compared to the ordered one.

Disregarding contributions due to the order-disorder transition c_v^{el} has been derived from the high-temperature c_p data, since the Invar anomalies are known to vanish at $T \gg T_C$. In accordance with the theory, we find that the linear coefficient of the electronic specific heat γ of the ordered sample is larger than the respective value for the disordered alloy. Together with $(c_p - c_v)$ and the Debye contribution, which is determined from earlier low-temperature measurements, the knowledge of c_v^{el} allows for a separation of the magnetic specific heat. We show the existance of considerable magnetic contributions in the paramagnetic temperature range that decrease almost linearly with increasing temperature. A comparison with theoretical results at finite temperatures based on the well-established $T = 0$ band-structure calculations for ordered Fe_3Pt reveal that these paramagnetic contributions are due to spin fluctuations, which dominate the contemporarily occurring volume fluctuations. They originate from the energetic instability of the high-spin (HS) state, which is the magnetic ground state of Fe_3Pt,with respect to the low-spin (LS) state, known as magnetovolume instability (MVI).

However, a jump of the magnetic specific heat at T_C as predicted by the theory is not observed. Moreover, there are quantitative discrepancies between the experimental electronic specific heat and theoretical data on the electronic DOS at the Fermi level. Most probably this is due to the fact that neither our applied method of analysis nor any available theory correctly accounts for the mutual coupling of electrons and phonons, and the respective excitations.

From a comparison of the total measured specific heat with $c_p(T)$ of a fictitious nonmagnetic reference material, which does not exhibit any Invar anomaly, and a discussion of the respective Gibbs free enthalpies we have shown that the volume instable magnetism in $Fe_{72}Pt_{28}$ Invar is stabilized by an energy of about 1 mRy/atom. This is equal to the energetic difference between the HS state and the LS state in Fe_3Pt as predicted by theory. Moreover, it is comparable to the energetic stability of the fcc phase with respect to the bcc phase, $\Delta G^{\text{fcc-bcc}}(T = 0)$. These results on $Fe_{72}Pt_{28}$ resemble the well-established coincidence of the steep decrease of the magnetic transition temperatures and the increase of the martensite start temperatures M_S with decreasing valence electron concentration in a narrow region around $e/a \simeq 8.6$.[3]

We have also shown that the energy, which stabilizes the ordered phase with respect to the disordered one, $\Delta G^{\text{ord-dis}}(T = 0)$, is again comparable to $\Delta G^{\text{fcc-bcc}}(T = 0)$. These observations are in good agreement with theoretical findings, which reveal that disorder destabilizes the magnetism:[56] Ordered Fe_3Ni, for example, turns out to be ferromagnetic, while disordered Fe_3Ni is nonmagnetic. As can be seen from the phase diagram (Fig. 3) ordered $Fe_{72}Pt_{28}$ exhibits a larger Curie temperature than the disordered sample. Simultaneously, M_S^{dis} is larger than M_S^{ord}, thus revealing a reduced stability of the fcc austenite phase in disordered $Fe_{72}Pt_{28}$.

ACKNOWLEDGMENTS

We would like to thank Professor Dr. P. Entel, Professor Dr. K. Schwarz, and Professor Dr. D. Wagner for valuable discussions. This work was supported by the Deutsche Forschungsgemeinschaft within the Sonderforschungsbereich 166.

[1] E.F. Wassermann, in *Ferromagnetic Materials*, edited by K.H. Bushow and E.P. Wohlfarth (North-Holland, Amsterdam, 1990), Vol. VI, p. 240.
[2] E.F. Wassermann, M. Acet, and W. Pepperhoff, J. Magn. Magn. Mater. **90&91**, 126 (1990).
[3] E.F. Wassermann, J. Magn. Magn. Mater. **100**, 346 (1991).
[4] V.L. Moruzzi and P.M. Marcus, Phys. Rev. B **34**, 1784 (1986).
[5] V.L. Moruzzi, Phys. Rev. B **41**, 6939 (1990).
[6] E.G. Moroni and T. Jarlborg, Phys. Rev. B **41**, 9600 (1990).
[7] S. Matar, J. Teichmann, and P. Mohn, in *International Conference on the Physics of Transition Metals*, edited by P.M. Oppeneer and L. Kübler (World Scientific, Singapore, 1993), Vol. II, p. 691.
[8] P. Entel, E. Hoffmann, P. Mohn, K. Schwarz, and V.L. Moruzzi, Phys. Rev. B **47**, 8706 (1993).
[9] M. Uhl, L.M. Sandratskii, and J. Kübler, J. Magn. Magn. Mater. **103**, 314 (1992).
[10] M. Acet, H. Zähres, E.F. Wassermann, and W. Pepperhoff, Phys. Rev. B **49**, 6012 (1994).
[11] M. Acet, T. Schneider, H. Zähres, E.F. Wassermann, and W. Pepperhoff, J. Appl. Phys. **75**, 7015 (1994).
[12] T. Schneider, M. Acet, B. Rellinghaus, E.F. Wassermann, and W. Pepperhoff (unpublished).
[13] M.M. Abd-Elmeguid and H. Micklitz, Physica B **161**, 17 (1989).
[14] P. Entel and M. Schröter, J. Phys. (Paris) Colloq. C 9, Suppl. **12**, C8-293 (1988).
[15] P. Mohn and G. Hilscher, Phys. Rev. B **40**, 9126 (1989).
[16] P. Mohn, K. Schwarz, and D. Wagner, Phys. Rev. B **43**, 3318 (1991).
[17] M. Uhl, L.M. Sandratskii, and J. Kübler, Phys. Rev. B **50**, 291 (1994).
[18] *Thermophysical Properties of Matter, Vol. 4: Specific Heat, Metallic Elements and Alloys*, edited by Y.S. Touloukian

and E.H. Buyco (IFI/Plenum Data Corporation, New York, 1978), p. 102.
[19] W. Bendick and W. Pepperhoff, Acta Metall. **30**, 679 (1982).
[20] M. Braun and R. Kohlhaas, Phys. Status Solidi **12**, 429 (1965).
[21] T.G. Kollie, Rev. Sci. Instrum. **38**, 1452 (1967).
[22] F. Krauß, Z. Metallkde. **49**, 386 (1958).
[23] K. Sumiyama, M. Shiga, and Y. Nakamura, J. Phys. Soc. Jpn. **40**, 996 (1976).
[24] K. Sumiyama, Y. Emoto, M. Shiga, and Y. Nakamura, J. Phys. Soc. Jpn. **50**, 3296 (1981).
[25] K. Sumiyama, M. Shiga, M. Morioka, and Y. Nakamura, J. Phys. F **9**, 1665 (1979).
[26] K. Sumiyama, M. Shiga, and Y. Nakamura, Phys. Status Solidi A **76**, 747 (1983).
[27] G. Hausch, J. Phys. Soc. Jpn. **37**, 824 (1974).
[28] Y. Shen, I. Nakai, H. Maruyama, and O. Yamada, J. Phy. Soc. Jpn. **54**, 3915 (1985).
[29] T. Mizoguchi, M. Akimitsu, and S. Chikazumi, J. Phys. Soc. Jpn. **34**, 932 (1973).
[30] T. Sasaki and S. Chikazumi, J. Phys. Soc. Jpn. **46**, 1732 (1979).
[31] M. Umemoto and C.M. Wayman, Metallurg. Trans. **9A**, 891 (1978).
[32] A. Kussmann and G.v. Rittberg, Z. Metallkde. **41**, 470 (1950).
[33] H. Maruyama, J. Phys. Soc. Jpn. **55**, 2834 (1986).
[34] N. Schubert, Ph.D. thesis, Gerhard-Mercator-Universität Duisburg, 1994.
[35] E.F. Wassermann, N. Schubert, J. Kästner, and B. Rellinghaus, J. Magn. Magn. Mater. (to be published).
[36] W. Bendick, H.H. Ertl, and W. Pepperhoff, J. Phys. F **8**, 2525 (1978).
[37] W. Bendick and W. Pepperhoff, J. Phys. F **11**, 57 (1981).
[38] Y. Tanji, H. Asano, and H. Moriya, Sci. Rep. RITU A **24**, 205 (1973).
[39] W. Pepperhoff, unpublished results on the specific heat of $Fe_{75}Pt_{25}$.
[40] M. Hansen and K. Anderko, *Constitution of Binary Alloys*, 2nd ed. (McGraw-Hill, New York, 1958), p. 699.
[41] W. Sykes and F.W. Jones, Proc. R. Soc. London, Ser. A **157**, 213 (1936).
[42] H.B. Callen, *Thermodynamics* (Wiley, New York, 1960), p. 127.
[43] G. Hausch, J. Phys. Soc. Jpn. **37**, 819 (1974).
[44] K. Tajima, Y. Endoh, Y. Ishikawa, and W.G. Stirling, Phys. Rev. Lett. **37**, 519 (1976).
[45] G. Grimvall, *The Electron-Phonon Interaction in Metals* (North-Holland, Amsterdam, 1981), p. 2.
[46] H. Herper, C. Holtfort, and P. Entel (private communication).
[47] M. Podgórny, Physica B **161**, 110 (1989).
[48] J. Inoue and M. Shimizu, J. Phys. F **13**, 2677 (1983).
[49] The double peak structure for the disordered sample is probably unphysical and originates from the large size of the specific-heat sample ($\sim$ 230 g) allowing for a certain inhomogeneity of the order parameter. Therefore, the peak in the specific heat is broader than in the thermal expansion.
[50] G. Hausch, J. Magn. Magn. Mater. **92**, 87 (1990).
[51] P. Mohn, K. Schwarz, and D. Wagner, unpublished results.
[52] M. Schröter, P. Entel, and S.G. Mishra, J. Magn. Magn. Mater. **87**, 163 (1990).
[53] M. Podgórny (unpublished).
[54] C.A. Kuhnen and E.Z. Da Silva, Phys. Rev. B **46**, 8915 (1992).
[55] E. Hoffmann, H. Herper, P. Entel, S.G. Mishra, P. Mohn, and K. Schwarz, Phys. Rev. B **47**, 5589 (1994).
[56] H. Ebert, M. Schröter, G.G. Reddy, P. Entel, E. Hoffmann, and H. Akai (unpublished).